Bremsstrahlung of a quark propagating through a nucleus

Boris Z. Kopeliovich,[1,2] Andreas Schäfer,[4] and Alexander V. Tarasov[2,3]
[1]*Max-Planck Institut für Kernphysik, Postfach 103980, D-69029 Heidelberg, Germany*
[2]*Joint Institute for Nuclear Research, Dubna, 141980 Moscow Region, Russia*
[3]*Institut für Theoretische Physik der Universität, Philosophenweg 19, D-69120 Heidelberg, Germany*
[4]*Institut für Theoretische Physik, Universität Regensburg, B-93040 Regensburg, Germany*
(Received 1 September 1998)

The density of gluons produced in the central rapidity region of a heavy-ion collision is poorly known. We investigate the influence of the effects of quantum coherence on the transverse momentum distribution of photons and gluons radiated by a quark propagating through nuclear matter. We describe the case where the radiation time substantially exceeds the nuclear radius (the relevant case for RHIC and LHC energies), which is different from what is known as the Landau-Pomeranchuk-Migdal effect corresponding to an infinite medium. We find *suppression* of the radiation spectrum at small transverse photon(gluon) momentum k_T, but *enhancement* for $k_T > 1$ GeV. Any nuclear effects vanish for $k_T \geqslant 10$ GeV. Our results also allow us to calculate the k_T-dependent nuclear effects in prompt photon, light, and heavy (Drell-Yan) dilepton and hadron production. [S0556-2813(99)05003-7]

PACS number(s): 24.85.+p, 12.38.Bx, 12.38.Aw, 25.75.−q

I. INTRODUCTION

One of the major theoretical problems in relativistic heavy-ion physics is the reliable calculation of the gluon bremsstrahlung in the central rapidity region. It is one of the determining factors for the general dynamics of heavy-ion collisions, the approach to thermodynamic equilibrium, and the possible formation of a quark-gluon plasmalike state. This problem has been approached by a variety of ways. We do not want to discuss the relative drawbacks and merits of the various approaches here and we will only cite those which are directly related to ours.

In this paper we consider the bremsstrahlung of photons and gluons resulting from the interaction of a projectile quark with a nucleus for the case where the radiation time is much longer than the time needed to cross the nucleus. This radiation or formation time was introduced in Ref. [1] and can be presented as

$$t_f = \frac{\cosh y}{k_T} \approx \frac{2\omega}{k_T^2}, \tag{1}$$

where y, ω, and k_T are the rapidity, energy, and transverse momentum of the radiated quantum in the nuclear rest frame. Equation (1) assumes that the radiated energy is relatively small, i.e., $\omega \ll E_q$. It is easy to interpret the formation time (1) as the lifetime of a photon(gluon)-quark fluctuation [2] or as the time needed to distinguish a radiated quantum from the static field of the quark [3].

The total time for the bremsstrahlung is proportional to the initial energy and can therefore substantially exceed the time of interaction with the target [4]. Radiation continues even after the quark leaves the target. This part of radiation does not resolve multiple scattering processes. Only the total momentum transfer is important. This illuminating manifestation of coherence is along the lines of the well known Landau-Pomeranchuk-Migdal effect (LPM) for which long formation times can be treated. Note that the LPM effect corresponds to the opposite energy limit, when the radiation time is much shorter that the time of propagation through the medium. It was first suggested by Landau and Pomeranchuk [1] and investigated by Migdal [5] and has attracted much attention in recent years [3,6–9]. This regime applies only for the problem of energy loss in a medium, which is not the problem we discuss here. Our treatment should apply to the real situation in heavy-ion collisions at high energies. The relationships between the cited papers are complex. In a recent publication Baier *et al.* [10] have shown that their diagrammatic approach is in fact equivalent to that of Zakharov [8]. The latter is, however, physically far more intuitive and therefore lends itself more easily to a generalization to the case where the nuclei are not infinitely extended. In another recent paper, Kovchegov and Mueller [11] have undertaken the first attempt to calculate an in-medium modification of the transverse momentum distribution of gluon radiation. This paper also has elucidated the relation between the approaches of Refs. [7] and [9]. In the approach of Ref. [9] based on the use of the light-cone gauge the final state interactions summed up in Ref. [7] (in the covariant gauge) are effectively included in the light-cone wave function. These observations suggest that all three different approaches might be equivalent when followed carefully enough.

The main goal of this paper is to study the dependence of the effects of coherence on the transverse momentum of the radiated photon or gluon. We use the light-cone approach for radiation first suggested in Ref. [12] and developed in Refs. [13,8]. As it is based on an explicit treatment of the transverse coordinates it is easily adapted to our purpose. In addition it seems to be by far the most direct and elegant approach. We described this approach in Sec. II for both the photon and gluon bremsstrahlung. We establish a relation between the strength of the coherence effects and the transverse size of the Fock state containing the radiated quantum.

The second main result of our paper is the extension of the light-cone approach to calculations for differential cross

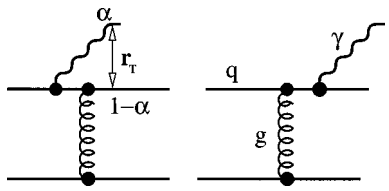

FIG. 1. Feynman graphs for electromagnetic bremsstrahlung.

sections as functions of the transverse photon(gluon) momentum $\vec{k}_T$. This is presented in Sec. III. As one might have expected, nuclear shadowing, i.e., *suppression* of radiation, is most pronounced at small k_T. An unexpected result is antishadowing, i.e., *enhancement* of radiation for $k_T > 1$ GeV, which, however, vanishes for still larger k_T.

The results and practical implications for the Drell-Yan process, prompt photon production, and hadroproduction are discussed in the last section.

II. INTEGRATED RADIATION SPECTRA

We start with electromagnetic radiation. We cover both virtual photon radiation (dilepton production) and real photon radiation (so called prompt photons).

The total radiation cross section for (virtual) photons, as calculated from the diagrams shown in Fig. 1, has the following factorized form in impact parameter representation [12] (see also Ref. [13]):

$$\frac{d\sigma^N(q\to\gamma q)}{d(\ln\alpha)} = \int d^2r_T |\Psi_{\gamma q}(\alpha,\vec{r}_T)|^2 \sigma_{\overline{qq}}(\alpha r_T). \quad (2)$$

Here $\Psi_{\gamma q}(\alpha,\vec{r}_T)$ is the wave function of the γ-q fluctuation of the projectile quark which depends on α, the relative fraction of the quark momentum carried by the photon, and r_T, the transverse separation between γ and q (Ψ is not normalized). $\sigma_{\overline{qq}}(\rho)$ is the total interaction cross section for a $\overline{q}q$ pair with transverse separation ρ and a nucleon. $\sigma_{\overline{qq}}(\rho)$ depends also parametrically on the total collision energy squared s, a dependence we do not write out explicitly (see, however, Sec. IV). This becomes only important when fits to actual data are performed. Equation (2) contains a remarkable observation which is crucial for this whole approach [12]: although we regard only a single projectile quark, the elastic amplitude of which is divergent, the *radiation* cross section is equal to the total cross section of a $\overline{q}q$ pair, which is finite.

This can be interpreted as follows. One should discriminate between the total interaction cross section and the freeing (radiation) cross section of a fluctuation. The projectile quark is represented in the light-cone approach as a sum of different Fock components. If each of them interacts with the target with the same amplitude the coherence between the components is not disturbed, i.e., no bremsstrahlung is generated. Therefore, the production amplitude of a new state (a new combination of the Fock components) is proportional to the difference between the elastic amplitudes of different fluctuations. Thus the universal divergent part of the elastic amplitudes cancels and the radiation amplitude is finite.

It is also easy to understand why the $\overline{q}q$ separation in Eq. (2) is αr_T. As is pointed out above one should take the difference between the amplitudes for a quark-photon fluctuation and a single quark. The impact parameters of these quarks are different. Indeed, the impact parameter of the projectile quark serves as the center of gravity for the γ-q fluctuation in the transverse plane. The distance to the quark in the quark-gluon Fock-state is then αr_T and that to the photon is $(1-\alpha)r_T$.

The wave function of the γq fluctuation in Eq. (2) for transversely and longitudinally polarized photons reads (compare with Ref. [14])

$$\Psi^{T,L}_{\gamma^* q}(\vec{r}_T,\alpha) = \frac{\sqrt{\alpha_{em}}}{2\pi}\overline{\chi_f}\hat{O}^{T,L}\chi_i K_0(\varepsilon r_T). \quad (3)$$

Here $\chi_{i,f}$ are the spinors of the initial and final quarks. $K_0(x)$ is the modified Bessel function. The operators $\hat{O}^{T,L}$ have the form

$$\hat{O}^T = i m_q \alpha^2 \vec{e}^* \cdot (\vec{n}\times\vec{\sigma}) + \alpha \vec{e}^* \cdot (\vec{\sigma}\times\vec{\nabla}) - i(2-\alpha)\vec{e}^* \cdot \vec{\nabla}, \quad (4)$$

$$\hat{O}^L = 2 m_{\gamma^*}(1-\alpha), \quad (5)$$

where

$$\varepsilon^2 = \alpha^2 m_q^2 + (1-\alpha) m_{\gamma^*}^2. \quad (6)$$

$\vec{e}$ is the polarization vector of the photon, $\vec{n}$ is a unit vector along the projectile momentum, and $\vec{\nabla}$ acts on $\vec{r}_T$. For radiation of prompt photons $m_{\gamma^*}=0$.

Equation (2) can be used for nuclear targets as well. We consider hereafter formation times given by the energy denominator

$$t_f = \frac{2E_q\alpha(1-\alpha)}{\epsilon^2 + m_q^2} \gg R_A, \quad (7)$$

which substantially exceed the nuclear radius. In this limit the transverse γ^*-q separation in the fluctuation is ''frozen,'' i.e., does not change during propagation through the nucleus. The recipe for the extension of Eq. (2) to a nuclear target is quite simple [12,15]. One should just replace $\sigma^N_{\overline{qq}}(\alpha r_T)$ by $\sigma^A_{\overline{qq}}(\alpha r_T)$:

$$\frac{d\sigma^A(q\to\gamma q)}{d(\ln\alpha)} = 2\int d^2b \int d^2r_T |\Psi_{\gamma q}(\alpha,\vec{r}_T)|^2 \times\left\{1-\exp\left[-\frac{1}{2}\sigma_{\overline{qq}}(\alpha r_T)T(b)\right]\right\}, \quad (8)$$

where

$$T(b) = \int_{-\infty}^{\infty} dz \rho_A(b,z). \quad (9)$$

Here $\rho_A(b,z)$ is the nuclear density which depends on the impact parameter b and the longitudinal coordinate z. One can eikonalize Eq. (2) because a fluctuation with a ''frozen'' transverse size is an eigenstate of interaction [15].

Equation (8) shows how the interference effects work versus k_T. At small r_T the exponent $\sigma_{\overline{qq}}(\alpha r_T)T(b)/2 \ll 1$ since

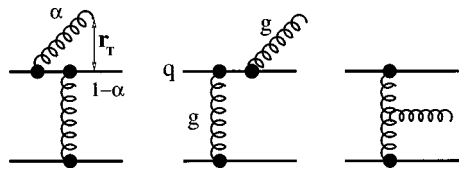

FIG. 2. Feynman graphs for gluon bremsstrahlung of an interacting quark.

$\sigma_{\bar{q}q}(\alpha r_T)$ is small. Therefore, one can expand the exponential and the cross section turns out to be proportional to A. This is the Bethe-Heitler limit for the bremsstrahlung. In the opposite limit $\sigma_{\bar{q}q}(\alpha r_T)T(b)/2 \gg 1$ one can neglect the exponential for $b \leqslant R_A$ and the cross section (8) is proportional to $A^{2/3}$. This is the limit of full coherence when the whole row of nucleons with the same impact parameter acts similar to a single nucleon. As the gluon transverse momentum is related to the inverse of r_T, one could expect that the limit of maximal coherence is reached for small k_T, and the Bethe-Heitler limit for large k_T. The situation is, however, more complicated as discussed in the next section.

Gluon radiation is described by the diagrams [16] shown in Fig. 2. The radiation cross section for a nucleon target and the nuclear effects [12] look similar to those of Eqs. (2)–(8),

$$\frac{d\sigma^A(q\to gq)}{d(\ln\alpha)} = 2\int d^2b \int d^2r_T |\Psi_{gq}(\alpha,\vec{r}_T)|^2 \times\left\{1-\exp\left[-\frac{1}{2}\sigma_{g\bar{q}q}(\vec{r}_1,\vec{r}_2)T(b)\right]\right\}, \tag{10}$$

where $\Psi_{gq}(\alpha,\vec{r}_T)$ is the wave function of a quark-gluon fluctuation which has the same form as Eq. (3), but with the replacements $\gamma^* \Rightarrow g$, $\alpha_{\rm em} \Rightarrow 4\alpha_s/3$, and $m_{\gamma^*} \Rightarrow m_g$. We keep the gluon mass nonzero in order to simulate the possible effects of confinement on gluon bremsstrahlung. $\sigma_{g\bar{q}q}$ is the interaction cross section of a colorless $g\bar{q}q$ system with a nucleon [17],

$$\sigma_{g\bar{q}q}(\vec{r}_1,\vec{r}_2) = \frac{9}{8}\{\sigma_{\bar{q}q}(r_1)+\sigma_{\bar{q}q}(r_2)\} - \frac{1}{8}\sigma_{\bar{q}q}(\vec{r}_1-\vec{r}_2), \tag{11}$$

where $\vec{r}_1$ and $\vec{r}_2$ are the transverse separations gluon-quark and gluon-antiquark, respectively. In the case of gluon radiation, i.e., Eq. (10), $\vec{r}_1=\vec{r}_T$ and $\vec{r}_2=(1-\alpha)\vec{r}_T$. Although Eq. (10) looks simple, it includes the effects of quark and gluon rescattering in the nucleus to all orders.

III. THE TRANSVERSE MOMENTUM DISTRIBUTION

A. Electromagnetic radiation

The transverse momentum distribution of photon bremsstrahlung in quark-nucleon interactions integrated over the final quark transverse momentum reads (see Appendix A)

$$\frac{d^3\sigma^N(q\to q\gamma)}{d(\ln\alpha)d^2k_T} = \frac{1}{(2\pi)^2}\int d^2r_1 d^2r_2 \times\exp[i\vec{k}_T(\vec{r}_1-\vec{r}_2)]\Psi^*_{\gamma q}(\alpha,\vec{r}_1) \times\Psi_{\gamma q}(\alpha,\vec{r}_2)\sigma_\gamma(\vec{r}_1,\vec{r}_2,\alpha), \tag{12}$$

where

$$\sigma_\gamma(\vec{r}_1,\vec{r}_2,\alpha) = \frac{1}{2}\{\sigma_{\bar{q}q}(\alpha r_1)+\sigma_{\bar{q}q}(\alpha r_2)-\sigma_{\bar{q}q}[\alpha(\vec{r}_1-\vec{r}_2)]\}. \tag{13}$$

By integrating over k_T one obviously recovers Eq. (2), since $\sigma_\gamma(\vec{r},\vec{r},\alpha)=\sigma_{\bar{q}q}(\alpha r)$.

For $\alpha \ll 1$ one can use the dipole approximation for the cross section, i.e., one can set $\sigma_{\bar{q}q}(\rho)=C\rho^2$. Moreover, this approximation also works rather well at larger interquark separations, even for hadronic sizes [18]. For the latter the cross section is proportional to the mean radius squared. Therefore, we use the dipole approximation for all cases considered. Then Eq. (13) simplifies to

$$\sigma_\gamma(\vec{r}_1,\vec{r}_2,\alpha) \approx C\alpha^2\vec{r}_1\cdot\vec{r}_2, \tag{14}$$

and we can explicitly calculate the k_T distribution (12),

$$\frac{d^3\sigma^N_T(q\to q\gamma^*)}{d(\ln\alpha)d^2k_T} = \frac{\alpha_{\rm em}}{\pi^2}\frac{C\alpha^2}{(k_T^2+\epsilon^2)^4}\{2m_q^2\alpha^4k_T^2 + [1+(1-\alpha)^2](k_T^4+\epsilon^4)\}, \tag{15}$$

$$\frac{d^3\sigma^N_L(q\to q\gamma^*)}{d(\ln\alpha)d^2k_T} = \frac{4\alpha_{\rm em}C\alpha^2(1-\alpha)^2m^2_{\gamma^*}k_T^2}{\pi^2(k_T^2+\epsilon^2)^4}. \tag{16}$$

Note that for small α Eqs. (15) and (16) vanish as does α^2. This could have been expected since electromagnetic bremsstrahlung is known to be located predominantly in the fragmentation regions of colliding particles rather than at midrapidity.

In the case of a nuclear target the transverse momentum distribution has to be modified by eikonalization of Eq. (12) (see Appendix A)

$$\frac{d^3\sigma^A(q\to q\gamma)}{d(\ln\alpha)d^2k_T} = \frac{1}{(2\pi)^2}\int d^2r_1 d^2r_2 \times\exp[i\vec{k}_T(\vec{r}_1-\vec{r}_2)]\Psi^*_{\gamma q}(\alpha,\vec{r}_1) \times\Psi_{\gamma q}(\alpha,\vec{r}_2)\Sigma_\gamma(\vec{r}_1,\vec{r}_2,\alpha), \tag{17}$$

where

$$\Sigma_\gamma(\vec{r}_1,\vec{r}_2,\alpha) = \int d^2b\left\{1+\exp\left[-\frac{1}{2}\sigma_{\bar{q}q}[\alpha(\vec{r}_1-\vec{r}_2)]T(b)\right] -\exp\left[-\frac{1}{2}\sigma_{\bar{q}q}(\alpha r_1)T(b)\right] -\exp\left[-\frac{1}{2}\sigma_{\bar{q}q}(\alpha r_2)T(b)\right]\right\}. \tag{18}$$

The fluctuation wave functions in Eq. (17) can be represented using Eq. (3) in the form

$$\sum_{\text{in},f} \Psi^T_{\gamma^* q}(\vec{r}_1,\alpha)\Psi^{T*}{}_{\gamma^* q}(\vec{r}_2,\alpha) = \frac{\alpha_{\text{em}}}{2\pi^2}\left\{ m_q^2\alpha^4 K_0(\varepsilon r_1)K_0(\varepsilon r_2) + [1+(1-\alpha)^2]\varepsilon^2\frac{\vec{r}_1\vec{r}_2}{r_1 r_2}K_1(\varepsilon r_1)K_1(\varepsilon r_2)\right\}, \quad (19)$$

$$\sum_{\text{in},f} \Psi^L_{\gamma^* q}(\vec{r}_1,\alpha)\Psi^{L*}{}_{\gamma^* q}(\vec{r}_2,\alpha) = \frac{2\alpha_{\text{em}}}{\pi^2} m^2_{\gamma^*}(1-\alpha)^2 K_0(\varepsilon r_1)K_0(\varepsilon r_2), \quad (20)$$

where we average over the initial quark polarization and sum over the final polarizations of quark and photon.

At first glance, one could think that the k_T distribution is not modified by the nucleus in the case $t_f \gg R_A$, since the fluctuation is formed long before the nucleus and the quark interact. This is, however, not the case. Due to color filtering [19] the mean size of $\overline{q}q$ dipoles surviving propagation through the nucleus decreases with A. Correspondingly, the transverse momentum of the photon increases. In other words, a heavier nucleus provides a larger momentum transfer to the quark, hence it is able to break up smaller size fluctuations and release photons with larger k_T.

Note that one can also calculate the distribution with respect to the transverse momentum $\vec{p}_T$ of the final quark integrating the differential cross section over the photon momentum $\vec{k}_T$. The result turns out to be the same as Eqs. (12) and (17) with the replacement $\alpha \Rightarrow 1-\alpha$.

We also calculated the nuclear dependence of the differential cross section (17), (18) using the dipole approximation for $\sigma_{\overline{q}q}(r)$. The details of the necessary integration can be found in Appendix B. As usual, we approximate the cross section by an A^n dependence. The power n is then defined by

$$n(k_T,\alpha) = \frac{d(\ln\{d^3\sigma^A(q\to q\gamma)/[d(\ln\alpha)d^2k_T]\})}{d(\ln A)}. \quad (21)$$

This power can also be A dependent. We performed calculations for $A=200$. To simplify these calculations, we used the constant density distribution, $\rho_A(r)=\rho_0\Theta(R_A-r)$ with $\rho_0 = 0.16\,\text{fm}^{-3}$.

First of all, we calculated $n(k_T,\alpha)$ for Drell-Yan lepton pair production at $m_{\gamma^*}=4$ GeV. The results are shown in Fig. 3 for transversely and longitudinally polarized virtual photons (the two components can be extracted from the angular distribution of the lepton pairs). We see that $n<1$ for $k_T<1$ GeV, i.e., the Drell-Yan pair production is shadowed by the nucleus. The shadowing is stronger for larger α [12]. Shadowing in the Drell-Yan process was first observed by the E772 Collaboration [20]. Their effect is, however, much weaker which can easily be explained because for Fermilab energies the radiation time (1) is quite short compared to the nuclear radius. This fact is taken into account in Ref. [12] by

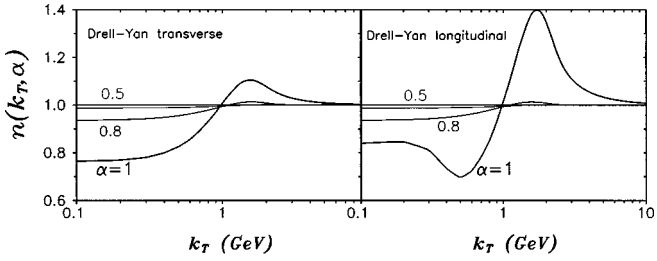

FIG. 3. The exponent (21) of the atomic number dependence parametrized as A^n versus k_T and α for transversely (left figure) and longitudinally (right figure) polarized virtual photons.

means of a nuclear form factor. Then the data can be described quite nicely (see also Ref. [21]).

An interesting result contained in Fig. 3 is the appearance of an antishadowing region for $k_T>1$ GeV. This is the first case in which the coherence effects enhance rather than suppress the radiation spectrum. It originates from an interference effect which is not noticeable for the integrated quantities.

Nuclear antishadowing is especially strong for longitudinal photons and $k_T \sim 1.5-2$ GeV. Color filtering in nuclear matter changes the angular distribution of Drell-Yan pairs and enhances the yield of longitudinally polarized dileptons. The nontrivial behavior of n for longitudinal photons at small k_T is due to the dip at $k_T=0$ in the differential cross section for a nucleon, see Eq. (16). This minimum is filled by multiple scattering of the quark in the nucleus leading to an increase of $n(k_T=0)$ and a strong A dependence of $n(k_T=0)$. [Formally, for longitudinal photons $n(k_T=0)$ goes to infinity for $A=1$, because the proton cross section at $k_T=0$ is zero.]

Note that nuclear enhancement of Drell-Yan pair production at large k_T was also observed experimentally [20]. However, as was mentioned, these data were taken in the kinematical region of the Bethe-Heitler regime, i.e., $t_f \ll R_A$. Therefore, they cannot be compared with our calculations. In fact the observation was explained quite satisfactory in Ref. [21].

The k_T dependence of n is expected to be nearly the same for different dilepton masses, down to the mass range probed in the CERES experiment at SPS CERN. However, the nuclear effects turn out to be quite different for real photons. Our results are shown in Fig. 4. In order to compare with experimental dilepton cross sections and prompt photon pro-

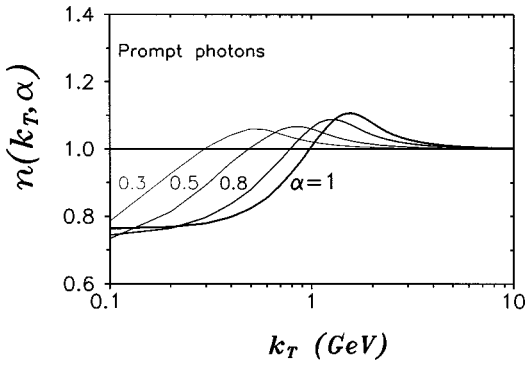

FIG. 4. The same as in Fig. 3, but for real photons.

duction rates our results have to be convoluted with the quark distribution function for the projectile proton. Since the electromagnetic radiation steeply falls off with decreasing α [proportional to α^2, see Eqs. (15), (16)], the convolution effectively picks out large values of α where the nuclear effects are in turn expected to be large. Detailed calculations and comparisons with data are postponed to a later publication.

B. Gluon radiation

Now we can discuss the bremsstrahlung in the non-Abelian case. Summing up the diagrams in Fig. 2 we get in impact parameter representation

$$\frac{d^3\sigma^N(q\to qg)}{d(\ln\alpha)d^2k_T}=\frac{1}{(2\pi)^2}\int d^2r_1d^2r_2 \times\exp[i\vec{k}_T(\vec{r}_1-\vec{r}_2)]\Psi^*_{gq}(\alpha,\vec{r}_1) \times\Psi_{gq}(\alpha,\vec{r}_2)\sigma_g(\vec{r}_1,\vec{r}_2,\alpha), \tag{22}$$

where (see Appendix A)

$$\sigma_g(\vec{r}_1,\vec{r}_2,\alpha)=\frac{1}{2}\{\sigma_{g\bar{q}q}(\vec{r}_1,\vec{r}_1-\alpha r_2)+\sigma_{g\bar{q}q}(\vec{r}_2,\vec{r}_2-\alpha r_1) -\sigma_{\bar{q}q}[\alpha(\vec{r}_1-\vec{r}_2)]-\sigma_{gg}(\vec{r}_1-\vec{r}_2)\}. \tag{23}$$

Here $\sigma_{gg}(r)=\frac{9}{4}\sigma_{\bar{q}q}(r)$ is the total cross section of a colorless gg dipole with a nucleon.

Note that Eq. (23) reproduces several simple limiting cases.

(1) $\sigma_g(\vec{r}_1,\vec{r}_2,\alpha)$ vanishes if either of r_1 or r_2 goes to zero, which expresses the fact that a pointlike quark-gluon fluctuation cannot be resolved by any interaction. To show this limiting behavior one simply has to insert, e.g., for $\vec{r}_2=0$, the two relations $\sigma_{g\bar{q}q}(\vec{r}_1,\vec{r}_1)=\sigma_{gg}(\vec{r}_1)$ and $\sigma_{g\bar{q}q}(\vec{0},-\alpha\vec{r}_1)=\sigma_{\bar{q}q}(-\alpha\vec{r}_1)=\sigma_{\bar{q}q}(\alpha\vec{r}_1)$. (Quark and antiquark at the same point in space act similar to a gluon.)

(2) For $\alpha\to1$ the quark-gluon separation tends to zero and Eq. (23) transforms into Eq. (13). On the other hand, at $\alpha\to0$ the quark-antiquark separation vanishes and Eq. (23) takes again the same form as Eq. (13), except that the $\bar{q}q$ pair is replaced by a gluon-gluon dipole:

$$\sigma_g(\vec{r}_1,\vec{r}_2,\alpha)\big|_{\alpha\ll1}=\frac{1}{2}\{\sigma_{gg}(r_1)+\sigma_{gg}(r_2)-\sigma_{gg}[(\vec{r}_1-\vec{r}_2)]\} =\frac{9}{4}\sigma_{\gamma^*}(\vec{r}_1,\vec{r}_2,\alpha)\big|_{\alpha=1}. \tag{24}$$

We use the dipole approximation $\sigma_{\bar{q}q}(r_T)\approx Cr_T^2$, which is well justified in this case since the mean transverse quark-gluon separation is small at small α. In this case Eqs. (23) and (11) lead to

$$\sigma_g(\vec{r}_1,\vec{r}_2,\alpha)\approx\left[\alpha^2+\frac{9}{4}(1-\alpha)\right]C\vec{r}_1\cdot\vec{r}_2. \tag{25}$$

This expression coincides with Eq. (14) up to the factor $[1+9(1-\alpha)/(4\alpha^2)]$. Therefore, we can use the results (15), (16) obtained for the photon bremsstrahlung which for $\alpha\to0$ lead to

$$\left.\frac{d^3\sigma_T^N(q\to qg)}{d(\ln\alpha)d^2k_T}\right|_{\alpha\ll1}\approx\frac{6C\alpha_s}{\pi^2}\frac{k_T^4+m_g^4}{(k_T^2+m_g^2)^4}, \tag{26}$$

$$\left.\frac{d^3\sigma_L^N(q\to gq)}{d(\ln\alpha)d^2k_T}\right|_{\alpha\ll1}\approx\frac{12C\alpha_sm_g^2k_T^2}{\pi^2(k_T^2+m_g^2)^4}. \tag{27}$$

In contrast to the photon bremsstrahlung these cross sections do not vanish for $\alpha\to0$. This is a consequence of the non-Abelian nature of QCD [16]. The radiating color current propagates through the whole rapidity interval between the projectile and the target providing a constant gluon density (26), (27) with respect to rapidity.

Eikonalization of the cross section (22) results in

$$\frac{d^3\sigma^A(q\to qg)}{d(\ln\alpha)d^2k_T}=\frac{1}{(2\pi)^2}\int d^2r_1d^2r_2 \times\exp[i\vec{k}_T(\vec{r}_1-\vec{r}_2)]\Psi^*_{gq}(\alpha,\vec{r}_1) \times\Psi_{gq}(\alpha,\vec{r}_2)\Sigma_g(\vec{r}_1,\vec{r}_2,\alpha), \tag{28}$$

where

$$\Sigma_g(\vec{r}_1,\vec{r}_2,\alpha)=\int d^2b\left\{\exp\left[-\frac{1}{2}\sigma_{\bar{q}q}[\alpha(\vec{r}_1-\vec{r}_2)]\right] +\exp\left[-\frac{1}{2}\sigma_{gg}(\vec{r}_1-\vec{r}_2)T(b)\right] -\exp\left[-\frac{1}{2}\sigma_{g\bar{q}q}(\vec{r}_1,\vec{r}_1-\alpha r_2)T(b)\right] -\exp\left[-\frac{1}{2}\sigma_{g\bar{q}q}(\vec{r}_2,\vec{r}_2-\alpha r_1)T(b)\right]\right\}. \tag{29}$$

In the limit $\alpha\ll1$, which is of practical interest at high energy, Eq. (23) transforms to the form of Eq. (24) and Eq. (29) simplifies to

$$\Sigma_g(\vec{r}_1,\vec{r}_2,\alpha)\big|_{\alpha\ll1}=\int d^2b\left\{1+\exp\left[-\frac{1}{2}\sigma_{gg}(\vec{r}_1-\vec{r}_2)T(b)\right] -\exp\left[-\frac{1}{2}\sigma_{gg}(\vec{r}_1)T(b)\right] -\exp\left[-\frac{1}{2}\sigma_{gg}(\vec{r}_2)T(b)\right]\right\}. \tag{30}$$

Note that the transverse momentum distribution for gluon radiation was calculated previously by Kovchegov and Mueller [11] in the limit $\alpha\to0$ and $m_q=m_g=0$. Our results (28), (30) agree with those in Ref. [11] in this limit and for the dipole approximation.

In Eq. (30) we make use of the fact that at zero $\bar{q}q$ separation a $g\bar{q}q$ system interacts similar to a pair of gluons, $\sigma_{g\bar{q}q}(\vec{r},\vec{r})=\sigma_{gg}(r)=(9/4)\sigma_{\bar{q}q}(r)$. Therefore, Eqs. (28), (29)

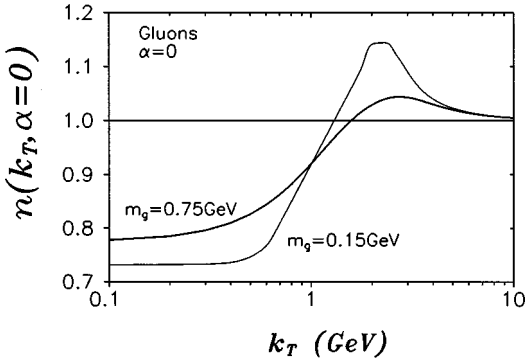

FIG. 5. The same as in Fig. 3, but for gluons at $\alpha=0$ for different effective gluon masses.

can be calculated in the same way as Eqs. (12)–(17) in the electromagnetic case at $\alpha=1$ (see Appendix B), except that the fluctuation wave functions must be taken at $\alpha=0$. We assign an effective mass to the gluon, either of the order of the inverse confinement radius, $m_g \approx 0.15\,\mathrm{GeV}$, or in accordance with the results of lattice calculations for the range of gluon-gluon correlations [22] of size $m_g=0.75\,\mathrm{GeV}$. We sum over the polarization of the emitted gluon. The numerical results are plotted in Fig. 5. They are qualitatively similar to those for photon radiation (see Fig. 3): shadowing at small and antishadowing at large k_T. However, the effect of antishadowing is more pronounced for light gluons.

Antishadowing of gluons results in antishadowing for inclusive hadron production, which is well known as the Cronin effect [23]. Although it was qualitatively understood that the source of this enhancement is multiple interaction of the partons in the nucleus, to our knowledge no realistic calculation taking into account color screening has been done so far. We expect that the Cronin effect disappears at very large k_T, which would actually be in accordance with available data [24]. For an honest comparison with these data, one has to relate the k_T of the gluon to that of the produced hadron, a step which lies not within the scope of this paper.

IV. CONCLUSIONS AND DISCUSSION

The main results of the paper are the following.

The factorized light-cone approach [12] for the analysis of radiation cross sections was extended to treat the k_T dependence, and was applied both to photon (real and virtual) and gluon bremsstrahlung.

The effects of coherence which are known to suppress radiation at long formation times, is only effective for small k_T. At $k_T>1$ GeV the interference instead actually enhances the radiation spectrum. This was indeed observed for dilepton and inclusive hadron production off nuclei (Cronin effect). The enhancement of radiation by the coherence effects turns out to vanish at very large transverse momenta $k_T \geqslant 10\,\mathrm{GeV}$. This was also observed in hadroproduction.

Suppression and enhancement of radiation by the effects of coherence are quite different for transversely and longitudinally polarized photons. Both contributions can be separated by measuring the angular distribution of the produced dileptons.

Note that we use Born graphs shown in Figs. 1 and 2 to derive expressions (2) and others having a factorized form. As a result of Born approximation the dipole cross section $\sigma_{\bar{q}q}(\rho)$ is energy independent. It is well known [28] that the higher order corrections lead to a cross section rising with energy. HERA data suggest that this energy dependence is correlated with the dipole size r_T. Therefore, the parameter $C(s)$ can be parametrized as

$$C(s)=C_0\left(\frac{s}{s_0}\right)^{\Delta(r_T)}, \tag{31}$$

where $s_0=100\,\mathrm{GeV}^2$, $C_0\approx 3$. The power $\Delta(r_T)$ grows with decreasing r_T. This dependence is extracted from an analysis of HERA data in Ref. [25]

Our results obtained for the radiation by a quark interacting with a nucleus are easily adapted to proton-nucleus collisions by convolution with the quark distribution in the proton. We plan also to extend our analysis to relativistic heavy-ion collisions. The condition we use, $t_f \gg R_A$, is poorly satisfied at present fixed target accelerators, but are well justified at RHIC or LHC. Indeed, if s_{NN} is the total NN collision energy squared, for a gluon(photon) radiated at central rapidity

$$\alpha=\frac{3k_T}{\sqrt{s_{NN}}}, \tag{32}$$

$$t_f=\frac{\sqrt{s_{NN}}}{m_N k_T}. \tag{33}$$

We conclude that at RHIC or LHC energies $\alpha \ll 1$ and that gluons with a few GeV transverse momentum are radiated far away from the nucleus, i.e., $t_f \gg R_A$. Thus our calculations should be directly applicable.

ACKNOWLEDGMENTS

We are grateful to Jörg Hüfner for many stimulating and fruitful discussions and to Vitali Dodonov for help with numerical calculations. We are especially thankful to Urs Wiedemann whose questions helped us to make the presentation more understandable. He also found a few misprints in Appendix A. The work of A.V.T. was supported by the Gesellschaft für Schwerionenforschung, GSI, Grant No. HD HÜF T, and A.S. was supported by the GSI Grant No. OR SCH T. A.V.T. and A.S. greatly acknowledge the hospitality of the MPI für Kernphysik.

APPENDIX A

In this appendix we illustrate how to eikonalize the differential cross section in the case of a nuclear target and for the example of the electromagnetic bremsstrahlung of an electron. The latter is described as propagating in a stationary field $U(\vec{x})$, where $\vec{x}$ is a three-dimensional vector.

The differential cross section reads

$$\frac{d^5\sigma}{d(\ln\alpha)d^2p_Td^2k_T}=\frac{\alpha_{\mathrm{em}}}{(2\pi)^4}|M_{fi}|^2, \tag{A1}$$

where $\vec{k}_T$ and $\vec{p}_T$ are the transverse momenta of the photon and the electron in the final state. The radiation amplitude for a transversely polarized massive photon $\gamma^*(\omega^2=k^2+m_{\gamma^*}^2)$ has the form

$$M_{fi}^T=\int d^3x\Psi^{-\dagger}(\vec{x},\vec{p}_2)\hat{\vec{\alpha}}\cdot\vec{e}^*e^{-i\vec{k}\vec{x}}\Psi^+(\vec{x},\vec{p}_1), \quad \text{(A2)}$$

where $\hat{\vec{\alpha}}=\gamma_0\vec{\gamma}$ are the Dirac matrices and the wave functions $\Psi(\vec{x},\vec{p}_{1,2})$ of the initial and final electron are solutions of the Dirac equation in the external potential $U(\vec{x})$,

$$[E_{1,2}-U(\vec{x})-m\beta+i\hat{\vec{\alpha}}\vec{\nabla}]\Psi(\vec{x},\vec{p}_{1,2})=0. \quad \text{(A3)}$$

The upper indices $-$ and $+$ in Eq. (A2) indicate that for the initial and final states the solutions contain in addition to the plane wave also an outgoing and incoming spherical wave, respectively. Using the Furry approximation [26] the solution of Eq. (A3) can be represented as

$$\Psi^+(\vec{x},\vec{p}_1)=e^{i|p_1|z}\hat{D}_1F^+(\vec{x},\vec{p}_1)\frac{u(\vec{p}_1)}{\sqrt{2E_1}}, \quad \text{(A4)}$$

$$\Psi^-(\vec{x},\vec{p}_2)=e^{i|p_2|z}\hat{D}_2F^-(\vec{x},\vec{p}_2)\frac{u(\vec{p}_2)}{\sqrt{2E_2}}, \quad \text{(A5)}$$

where $u(\vec{p}_{1,2})$ is the four-component spinor corresponding to a free electron with momentum $\vec{p}_{1,2}$

$$\hat{D}_{1,2}=1-i\frac{\hat{\vec{\alpha}}\cdot\vec{\nabla}}{2E_{1,2}}-\frac{\hat{\vec{\alpha}}\cdot\vec{p}_{1,2T}}{2E_{1,2}}. \quad \text{(A6)}$$

The scalar functions $F(\vec{x},\vec{p})$ in Eqs. (A4), (A5) are the solutions of the two-dimensional Schrödinger equation

$$i\frac{d}{dz}F(\vec{x},\vec{p})=\left[-\frac{\Delta_T}{2p}+U(\vec{x})\right]F(\vec{x},\vec{p}), \quad \text{(A7)}$$

where $p=|\vec{p}|$. We define $F^{\pm}$ in accordance with the asymptotic behavior

$$F^+(\vec{x},\vec{p}_1)|_{z\to z_-=-\infty}\to e^{i\vec{p}_{1T}\vec{r}}, \quad \text{(A8)}$$

$$F^-(\vec{x},\vec{p}_2)|_{z\to z_+=+\infty}\to e^{i\vec{p}_{2T}\vec{r}}. \quad \text{(A9)}$$

Here we introduced new notations for transverse, $\vec{r}\equiv\vec{x}_T$, and longitudinal, $z\equiv x_L$, coordinates.

It follows from Eqs. (A7)–(A9) that these functions can be represented in the form

$$F^+(\vec{x},\vec{p}_1)=\int d^2r_1G(z,\vec{r};z_-,\vec{r}_1|\vec{p}_1)e^{i\vec{p}_{1T}\vec{r}_1}, \quad \text{(A10)}$$

$$F^{-*}(\vec{x},\vec{p}_2)=\int d^2r_2G(z_+,\vec{r}_2;z,\vec{r}|\vec{p}_2)e^{-i\vec{p}_{2T}\vec{r}_2}, \quad \text{(A11)}$$

where $G(z_2,\vec{r}_2;z_1,\vec{r}_1|\vec{p})$ is the retarded Green function corresponding to Eq. (A7),

$$\left[i\frac{d}{dz_2}+\frac{\Delta_2}{2p}-U(z_2,\vec{r}_2)\right]G(z_2,\vec{r}_2;z_1,\vec{r}_1|\vec{p})=i\delta(z_2-z_1)\delta(\vec{r}_2-\vec{r}_1) \quad \text{(A12)}$$

and satisfying the conditions

$$G(z_2,\vec{r}_2;z_1,\vec{r}_1|\vec{p})|_{z_1=z_2}=\delta(\vec{r}_2-\vec{r}_1),$$

$$G(z_2,\vec{r}_2;z_1,\vec{r}_1|\vec{p})|_{z_1>z_2}=0. \quad \text{(A13)}$$

It is convenient to choose the axis z along the momentum of the radiated photon. Then

$$\vec{p}_{1T}=-\frac{\vec{k}_T}{\alpha},$$

$$\vec{p}_{2T}=\vec{p}_T-\frac{1-\alpha}{\alpha}\vec{k}_T, \quad \text{(A14)}$$

where $\vec{k}_T$ and $\vec{p}_T$ are the transverse components of the photon and final electron momenta relative to the direction of the initial electron; α is the fraction of the light-cone momentum of the initial electron carried by the photon.

We arrive at the following expression for the radiation amplitude (A2):

$$M_{fi}^T=\frac{1}{2p(1-\alpha)}\int d^2r_1d^2r_2d^2rdz\times\exp(-i\vec{p}_{2T}\vec{r}_2)G(z_+,r_2;z,r|\vec{p}_2)\times\exp(iq_{\min}z)\hat{\Gamma}G(z,r;z_-,r_1|\vec{p}_1)\exp(i\vec{p}_{1T}\vec{r}_1), \quad \text{(A15)}$$

where

$$q_{\min}=\frac{\alpha m^2}{2(1-\alpha)E}+\frac{m_{\gamma^*}^2}{2\alpha E}, \quad \text{(A16)}$$

and E,m are the energy and the mass of the projectile electron. In the approximation considered in this paper when the fluctuation time substantially exceeds the interaction time, $q_{\min}\ll 1/R_A$ and can be neglected.

The vertex function in Eq. (A15) reads

$$\hat{\Gamma}=\sqrt{1-\alpha}u^*(\vec{p}_2)\hat{D}_2^*\hat{\vec{\alpha}}\cdot\vec{e}^*\hat{D}_1u(p_1)=\chi_2^\dagger[im\alpha(\vec{n}\times\vec{\sigma})\cdot\vec{e}^*+\alpha(\vec{\sigma}\times\vec{\nabla}_T)\cdot\vec{e}^*-i(2-\alpha)\vec{\nabla}_T\cdot\vec{e}^*]\chi_1. \quad \text{(A17)}$$

The operator $\vec{\nabla}_T=d/d\vec{r}$ acts to the right. $\chi_{1,2}$ are the two-component spinors of the initial and final electrons.

In the case of a composite target the potential has to be summed over the constituents

$$U(\vec{r},z)=\sum_i U_0(\vec{r}-\vec{r}_i,z-z_i) \quad \text{(A18)}$$

and the bremsstrahlung cross section should be averaged over the positions $(\vec{r}_i,z_i)$ of the scattering centers.

The averaged matrix element squared takes the form

$$\langle |M_{fi}^{T}|^2\rangle = 2\,\mathrm{Re}\int_{-\infty}^{\infty} dz_1 \int_{z_1}^{\infty} dz_2 \int d^2r_1 d^2r_1' d^2r_2 d^2r_2' d^2r d^2r' d^2\rho d^2\rho'$$
$$\times \exp[i\vec{p}_{2T}(\vec{r}_2'-\vec{r}_2) - i\vec{p}_{1T}(\vec{r}_1'-\vec{r}_1) - iq_{\min}(z_2-z_1)]$$
$$\times \langle G(z_+,\vec{r}_2;z_2,\vec{\rho}|p_2) G^*(z_+,\vec{r}_2';z_2,\vec{r}'|p_2)\rangle$$
$$\times \hat{\Gamma}'^* \langle G(z_2,\vec{\rho};z_1,\vec{r}|p_2) G^*(z_2,\vec{r}';z_1,\vec{\rho}'|p_1)\rangle$$
$$\times \hat{\Gamma} \langle G(z_1,\vec{r};z_-,\vec{r}_1|p_1) G^*(z_1,\vec{\rho}';z_-,\vec{r}_1'|p_1)\rangle, \tag{A19}$$

where $\hat{\Gamma}'$ differs from $\hat{\Gamma}$ in Eq. (A17) by the replacement

$$\vec{\nabla} = \frac{d}{d\vec{r}} \Rightarrow \vec{\nabla}' = \frac{d}{d\vec{r}'}.$$

The following consideration is based on the representation of the Green function G in the form of a continuous integral [27]:

$$G(z_2,\vec{r}_2;z_1,\vec{r}_1|p) = \int \mathcal{D}\vec{r}(z) \exp\left\{ \frac{ip}{2}\int_{z_1}^{z_2} dz \left(\frac{d\vec{r}(z)}{dz}\right)^2 - i\int_{z_1}^{z_2} dz\, U[\vec{r}(z),z]\right\}, \tag{A20}$$

where

$$\vec{r}(z_1)=\vec{r}_1, \quad \vec{r}(z_2)=\vec{r}_2,$$

and the relation

$$\int_{z_1}^{z_2} dz \sum_i U_0(\vec{r}(z)-\vec{r}_i, z-z_i) = \sum_i \chi[\vec{r}(z_i)-\vec{r}_i]\Theta(z_2-z_i)\Theta(z_i-z_1), \tag{A21}$$

where $\chi(\vec{r}) = \int_{-\infty}^{\infty} dz\, U_0(\vec{r},z)$. The mean value of the eikonal exponential is

$$\left\langle \exp\left\{ i\sum_i \{\chi[\vec{r}(z_i)] - \chi[\vec{r}'(z_i)]\}\Theta(z_2-z_i)\Theta(z_i-z_1)\right\}\right\rangle = \exp\left\{ -\frac{1}{2}\int_{z_1}^{z_2} dz\, n(z,\vec{b})\sigma[\vec{r}(z)-\vec{r}'(z)]\right\}, \tag{A22}$$

where

$$\sigma(\vec{r}-\vec{r}') = 2\int d^2\rho\{1-\exp[i\chi(\vec{r}-\vec{\rho}) - i\chi(\vec{r}'-\vec{\rho})]\}, \tag{A23}$$

and $n(z,\vec{b})$ is the density of scattering centers.

Using these relations and performing integration by parts in Eq. (A19),

$$\frac{d\sigma^T}{d(\ln\alpha)d^2p_T d^2k_T} = \frac{\alpha_{\mathrm{em}}}{(2\pi)^4 4p^2(1-\alpha)^2} 2\,\mathrm{Re}\int_{-\infty}^{\infty} dz_1 \int_{z_1}^{\infty} dz_2 \int d^2b\, d^2\rho_1 d^2\rho_2$$
$$\times \exp\left[i\alpha\vec{p}_{2T}\vec{\rho}_2 - i\alpha\vec{p}_{1T}\vec{\rho}_1 - \int_{z_2}^{0} dz V(z,\vec{\rho}_2) - \int_{-\infty}^{z_1} dz V(z,\vec{\rho}_1)\right]$$
$$\times \hat{\gamma}_2 \hat{\gamma}_1^* W(z_2,\vec{\rho}_2;z_1,\vec{\rho}_1|\rho). \tag{A24}$$

The variables in this equation are related to those in Eq. (A19) as

$$\vec{\rho}_1 = \frac{\vec{r}_1'-\vec{r}_1}{\alpha},$$

$$\vec{\rho}_2 = \frac{\vec{r}_2'-\vec{r}_2}{\alpha},$$

$$\vec{b} = \frac{1}{2}(\vec{r}_1'+\vec{r}_1).$$

Other variables in Eq. (A19) are integrated explicitly.

Matrices $\hat{\gamma}$ are related to $\hat{\Gamma}$ in Eq. (A17) by replacement $m \Rightarrow \alpha m$ and $d/d\vec{r} \Rightarrow d/d\vec{\rho}$.

Absorptive potential V in Eq. (A24) reads

$$V(z,\vec{\rho}) = n(z,\vec{b})\frac{\sigma}{2}(\alpha\cdot\vec{\rho})$$

and W is the solution of either of the equations

$$\frac{\partial}{\partial z_2} W(z_2,\vec{\rho}_2;z_1,\vec{\rho}_1|p) = \frac{i[\Delta(\vec{\rho}_2)-\varepsilon^2]}{2\alpha(1-\alpha)p} W(z_2,\vec{\rho}_2;z_1,\vec{\rho}_1|p) - V(\vec{\rho}_2,z_2) W(z_2,\vec{\rho}_2;z_1,\vec{\rho}_1|p), \tag{A25}$$

$$-\frac{\partial}{\partial z_1} W(z_2,\vec{\rho}_2;z_1,\vec{\rho}_1|p) = \frac{i[\Delta(\vec{\rho}_1)-\varepsilon^2]}{2\alpha(1-\alpha)p} W(z_2,\vec{\rho}_2;z_1,\vec{\rho}_1|p) - V(\vec{\rho}_1,z_1) W(z_2,\vec{\rho}_2;z_1,\vec{\rho}_1|p), \tag{A26}$$

with the boundary condition

$$W(z_2,\vec{\rho}_2;z_1,\vec{\rho}_1|p)\big|_{z_2=z_1} = \delta(\vec{\rho}_2-\vec{\rho}_1). \tag{A27}$$

Using these equations and the relation

$$[\Delta(\vec{\rho})-\varepsilon^2] K_0(\varepsilon|\vec{\rho}|) = -2\pi\delta(\vec{\rho}), \tag{A28}$$

simple but cumbersome calculations lead to a new form for Eq. (A24),

$$\begin{aligned}
\frac{d\sigma^T}{d(\ln\alpha)d^2p_T d^2k_T} = \frac{\alpha^2}{(2\pi)^4}\Bigg\{ & \mathrm{Re}\int_{-\infty}^{\infty} dz \int d^2b\, d^2\rho_1 d^2\rho_2 d^2\rho \\
& \times \exp\left[i\alpha\vec{p}_{2T}\vec{\rho}_2 - i\alpha\vec{p}_{1T}\vec{\rho}_1 - \int_z^{\infty} dz' V(z',\vec{\rho}_2) - \int_{-\infty}^{z} dz' V(z',\vec{\rho}_1) \right] \\
& \times \Psi_T^{\dagger}(\vec{\rho}_2-\vec{\rho})[2V(z,\vec{\rho}) - V(z,\vec{\rho}_1) - V(z,\vec{\rho}_2)]\Psi_T(\vec{\rho}_1-\vec{\rho}) \\
& - 2\,\mathrm{Re}\int_{-\infty}^{\infty} dz_1 \int_{z_1}^{\infty} dz_2 \int d^2b\, d^2\rho_1 d^2\rho_2 d^2\rho_1' d^2\rho_2' \\
& \times \exp\left[i\alpha\vec{p}_{2T}\vec{\rho}_2 - i\alpha\vec{p}_{1T}\vec{\rho}_1 - \int_{z_2}^{\infty} dz V(z,\vec{\rho}_2) - \int_{-\infty}^{z_1} dz V(z,\vec{\rho}_1) \right] \Psi_T^{\dagger}(\vec{\rho}_2-\vec{\rho}_2') \\
& \times [V(z_2,\vec{\rho}_2) - V(z_2,\vec{\rho}_2')] W(z_2,\vec{\rho}_2';z_1,\vec{\rho}_1'|p)[V(z_1,\vec{\rho}_1) - V(z_1,\vec{\rho}_1')]\Psi_T(\vec{\rho}_1-\vec{\rho}_1') \Bigg\},
\end{aligned} \tag{A29}$$

where

$$\Psi_T(\vec{\rho}) = \frac{\sqrt{\alpha_{\mathrm{em}}}}{2\pi}\hat{\Gamma} K_0(\epsilon\rho). \tag{A30}$$

In the ultrarelativistic limit ($p\to\infty$) we have

$$W(z_2,\vec{\rho}_2;z_1,\vec{\rho}_1|\infty) = \delta(\vec{\rho}_2-\vec{\rho}_1)\exp\left[-\int_{z_1}^{z_2} dz V(z,\vec{\rho}_2)\right]. \tag{A31}$$

The integrations over z, z_1, z_2 in Eq. (A29) can be performed analytically, and we arrive at the expression

$$\begin{aligned}
\frac{d\sigma^T}{d(\ln\alpha)d^2p_T d^2k_T} = \frac{\alpha^2}{(2\pi)^4}\int d^2r_1 d^2r_2 d^2r\, \exp[i\alpha\vec{r}(\vec{p}_T+\vec{k}_T) + i(\vec{r}_1-\vec{r}_2)\vec{k}_T]\psi_T(\vec{r}_1)\psi_T^*(\vec{r}_2) \\
\times\{\Sigma[\alpha(\vec{r}+\vec{r}_1)] + \Sigma[\alpha(\vec{r}-\vec{r}_2)] - \Sigma(\alpha\vec{r}) - \Sigma[\alpha(\vec{r}+\vec{r}_1-\vec{r}_2)]\},
\end{aligned} \tag{A32}$$

where

$$\Sigma(\rho) = \int d^2b \left\{ 1 - \exp\left[-\frac{\sigma(\rho)}{2} T(b)\right]\right\}. \tag{A33}$$

The derivation of the correspondent expressions for gluon bremsstrahlung was done analogously. It does not contain any really new feature, and the expressions are too long to be displayed in detail.

APPENDIX B

In order to calculate Eqs. (17), (18) in the dipole approximation $\sigma_{q\bar{q}}=Cr^2$, we need to evaluate integrals of two types:

$$I_1=\frac{1}{(2\pi)^2}\int d^2r_1 d^2r_2\exp[i\vec{k}_T(\vec{r}_1-\vec{r}_2)]K_0(\varepsilon r_1)\times K_0(\varepsilon r_2)\exp\left\{-\frac{1}{4}(fr_1^2+hr_2^2-2g\vec{r}_1\vec{r}_2)\right\} \quad \text{(B1)}$$

and

$$I_2=\frac{1}{(2\pi)^2}\int d^2r_1 d^2r_2\exp[i\vec{k}_T(\vec{r}_1-\vec{r}_2)]\times\frac{(\vec{r}_1\vec{r}_2)}{r_1r_2}K_1(\varepsilon r_1)K_1(\varepsilon r_2)\times\exp\left\{-\frac{1}{4}(fr_1^2+hr_2^2-2g\vec{r}_1\vec{r}_2)\right\}. \quad \text{(B2)}$$

Here we use the notation

$$\frac{\sigma_{q\bar{q}}(\rho)}{2}T(b)=\frac{1}{4}(fr_1^2+hr_2^2-2g\vec{r}_1\vec{r}_2). \quad \text{(B3)}$$

We use the integral representation for the modified Bessel functions, which reads

$$K_0(\varepsilon r)=\frac{1}{2}\int_0^\infty\frac{dt}{t}\exp\left\{-t-\frac{\varepsilon^2r^2}{4t}\right\}, \quad \text{(B4)}$$

$$\frac{1}{\varepsilon r}K_1(\varepsilon r)=\frac{1}{4}\int_0^\infty\frac{dt}{t^2}\exp\left\{-t-\frac{\varepsilon^2r^2}{4t}\right\}. \quad \text{(B5)}$$

After substitution of Eqs. (B4) and (B5) into (B1) and (B2) and making use of the following obvious relations:

$$I_3=\frac{1}{4(2\pi)^2}\int d^2r_1 d^2r_2\exp\left\{i\vec{k}_T(\vec{r}_1-\vec{r}_2)-\frac{1}{4}(ar_1^2+cr_2^2-2b\vec{r}_1\vec{r}_2)\right\}=\frac{1}{(ac-b^2)}\exp\left\{-\frac{k_T^2(a+c-2b)}{(ac-b^2)}\right\}, \quad \text{(B6)}$$

$$I_4=\frac{1}{16(2\pi)^2}\int d^2r_1 d^2r_2(\vec{r}_1\vec{r}_2)\exp\left\{i\vec{k}_T(\vec{r}_1-\vec{r}_2)-\frac{1}{4}(ar_1^2+cr_2^2-2b\vec{r}_1\vec{r}_2)\right\}=\left[\frac{b}{(ac-b^2)^2}-\frac{k_T^2(a-b)(c-d)}{(ac-b^2)^3}\right]\times\exp\left\{-\frac{k_T^2(a+c-2b)}{ac-b^2}\right\} \quad \text{(B7)}$$

one arrives at

$$I_1=\int\frac{dt}{t}\frac{du}{u}\exp(-u-t)I_3,$$

$$I_2=\varepsilon^2\int\frac{dtdu}{t^2u^2}\exp(-u-t)I_4, \quad \text{(B8)}$$

where

$$a=\frac{\varepsilon^2}{t}+f,\quad c=\frac{\varepsilon^2}{u}+h,\quad b=g. \quad \text{(B9)}$$

Thus, for the general case in addition to the integration over the impact parameter one has to evaluate numericaly a two-dimensional integral over *dt* and *du*.

The situation is simplified in the case of photon bremsstrahlung, when integration for the three exponentials in Eq. (17) corresponds to the following values of the parameters, respectively:

$$f=g=0,\quad h=2c\alpha^2T(b),$$

$$h=g=0,\quad f=2c\alpha^2T(b),$$

$$f=h=g=2c\alpha^2T(b). \quad \text{(B10)}$$

In this case Eqs. (B8) are reduced to one-dimensional integrals.

[1] L. D. Landau and I. Ya. Pomeranchuk, Zh. Eksp. Teor. Fiz. **24**, 505 (1953); Dokl. Akad. Nauk SSSR **92**, 535 (1953); **92**, 735 (1953); E. L. Feinberg and I. Ya. Pomeranchuk, *ibid.* **93**, 439 (1953); I. Ya. Pomeranchuk, *ibid.* **96**, 265 (1954); **96**, 481 (1954); E. L. Feinberg and I. Ya. Pomeranchuk, Nuovo Cimento Suppl. **4**, 652 (1956).

[2] B. Z. Kopeliovich, J. Nemchik, and E. Predazzi, *Hadronization in Nuclear Environment and Electroproduction of Leading Hadrons*, in Proceedings of ELFE Summer School on Confinement Physics, edited by S. D. Bass and P. A. M. Guichon (Editions Frontieres, Gif-sur-Yvette, France, 1995), p. 391, hep-ph/9511214.

[3] M. Gyulassy and X.-N. Wang, Nucl. Phys. **B420**, 583 (1994); M. Gyulassy and M. Plümer, Phys. Rev. D **51**, 3436 (1995).

[4] See, e.g., Yu. L. Dokshitzer, V. A. Khoze, A. H. Mueller, and S. I. Troyan, *Basics of Perturbative QCD* (Editions Frontieres, Gif-sur-Yvette, France, 1991), Chap. 1.

[5] A. B. Migdal, Phys. Rev. **103**, 1811 (1956).

[6] F. Niedermayer, Phys. Rev. D **34**, 3494 (1986).

[7] R. Baier, Yu. L. Dokshitzer, A. H. Mueller, S. Peigne, and D.

Schiff, Nucl. Phys. **B483**, 291 (1997); **B484**, 265 (1997).
[8] B. G. Zakharov, JETP Lett. **63**, 952 (1996); **64**, 781 (1996); **65**, 615 (1997).
[9] J. Jalilian-Marian, A. Kovner, L. Mc Lerran, and H. Weigert, Phys. Rev. D **55**, 5414 (1997).
[10] R. Baier, Yu. L. Dokshitzer, A. H. Mueller, and D. Schiff, hep-ph/9804212.
[11] Y. V. Kovchegov and A. H. Mueller, Nucl. Phys. **B529**, 451 (1998).
[12] B. Z. Kopeliovich, Soft Component of Hard Reactions and Nuclear Shadowing (DIS, Drell-Yan reaction, heavy quark production), in Proceedings of the Workshop Hirschegg'95: Dynamical Properties of Hadrons in Nuclear Matter, Hirschegg, 1995, edited by H. Feldmeier and W. Nörenberg, Darmstadt, 1995, hep-ph/9609385, p. 102.
[13] S. J. Brodsky, A. Hebecker, and E. Quack, Phys. Rev. D **55**, 2584 (1997).
[14] J. B. Kogut and D. E. Soper, Phys. Rev. D **1**, 2901 (1970); J. M. Bjorken, J. B. Kogut, and D. E. Soper, *ibid.* **3**, 1382 (1971).
[15] A. B. Zamolodchikov, B. Z. Kopeliovich, and L. I. Lapidus, JETP Lett. **33**, 595 (1981).
[16] J. F. Gunion and G. Bertsch, Phys. Rev. D **25**, 746 (1982).
[17] N. N. Nikolaev and B. G. Zakharov, JETP **78**, 598 (1994).
[18] J. Hüfner and B. Povh, Phys. Rev. D **46**, 990 (1992).
[19] G. Bertsch, S. J. Brodsky, A. S. Goldhaber, and J. F. Gunion, Phys. Rev. Lett. **47**, 297 (1981).
[20] D. M. Alde *et al.*, Phys. Rev. Lett. **64**, 2479 (1990).
[21] J. Hüfner and B. Z. Kopeliovich, Phys. Lett. B **312**, 235 (1993).
[22] E. V. Shuryak, Rev. Mod. Phys. **65**, 1 (1993).
[23] J. Cronin *et al.*, Phys. Rev. Lett. **31**, 426 (1973).
[24] Y. B. Hsiung *et al.*, Phys. Rev. Lett. **55**, 457 (1985).
[25] B. Z. Kopeliovich and B. Povh, hep-ph/9806284.
[26] W. N. Furry, Phys. Rev. **46**, 391 (1934).
[27] R. P. Feynman and A. R. Gibbs, *Quantum Mechanics and Path Integrals* (McGraw-Hill, New York, 1965).
[28] L. N. Lipatov, Sov. Phys. JETP **63**, 904 (1986).